The vertical dotted lines represent typical ratios of maximum torque to moment of inertia for satellites in the 500- to 1500-lb class. The weight of the power supply for an ion propulsion attitude-control system for such satellites will be less than 10 lb (Fig. 10). In the semicontinuous North-South mode of operation, the engines are operated directly from the solar cells so that no energy storage system is needed for the station-keeping system. However, about 30 w-hr of energy storage capability will be required to operate the attitude-control engines during the time the vehicle spends in the earth's shadow (a maximum of 1.16 hr/day). Typical attitude-control and station-keeping system weights required for a 1000-lb vehicle when using the continuous station-keeping thrust mode are shown in Table 4.

Conclusions

Three-axes attitude control and station keeping of a stationary satellite are well within the capabilities of ion propulsion systems. Some of the problems peculiar to this application of ion engines, such as the need for extremely low ionizer warmup energy, are already near solution, and others, such as engine reliability after thousands of thrust pulses, will be accomplished and demonstrated in the near future. A prototype system of the type described in this paper has been developed and laboratory tested. A comparison of the weights of several types of attitude-control and station-keeping systems (as discussed by Boucher[2]) has shown that as the desired lifetime of satellites extends to more than one year, the ion propulsion system emerges as the lightest attitude-control and station-keeping system presently under development.

References

[1] McElvain, R. J., "Effects of solar radiation pressure upon satellite attitude control," ARS Preprint 1918-61 (August 1961).

[2] Boucher, R. A., "Electrical propulsion for control of stationary satellites," J. Spacecraft Rockets 1, 164–169(1964).

[3] Ehricke, K. A., "Dynamics," *Space Flight* (D. Van Nostrand, Inc., Princeton, N. J., 1962), Vol. II, pp. 144–150.

[4] Jensen, J., Townsend, G. E., Kraft, J. D., and Kork, J., *Design Guide to Orbital Flight* (McGraw-Hill Book Co., Inc., N. Y., 1962), p. 138.

[5] Molitor, J. H. and Kaplan, M. H., "Optimization of ion engine control systems for synchronous satellites," AIAA Preprint 63-273 (June 1963).

MARCH-APRIL 1964 J. SPACECRAFT VOL. 1, NO. 2

Fluxgate Magnetometer for Space Application

S. C. LING*
Therm, Inc., Ithaca, N. Y.

A new type of fluxgate magnetometer based on the principle of minimum flux linkage between the gating field and the ambient field is developed for space application wherein field strengths of the order of a few gammas are to be detected. Through the unique combination of several physical properties of the magnetometer, a stable decoupling factor of the order of 10^{-7} is achieved. A phenomenological theory is presented to explain the general mechanics of the fluxgate, and a discussion of the spectrum of transverse induction is made. Experimental values for a typical magnetometer and its circuitry are presented in order to demonstrate its working principle.

Introduction

AN advanced type of fluxgate magnetometer was developed for space applications, in which magnetic field strengths of the order of a few gammas ($1\gamma = 10^{-5}$ gauss) are to be detected. In order to measure such weak fields, one must find a way to minimize effects of the disturbances due to the presence of the space vehicle and its associated controls and instruments. Realizing this fact, T. Gold urged the development of a magnetometer sufficiently small and sensitive to be attached to the end of a boom 20 to 30 ft away from the vehicle, so that the disturbing magnetic field would be reduced to an acceptable level according to the inverse-distance-cubed law. This concept led to the development of an improved fluxgate magnetometer, which is described in this paper.

In general, a fluxgate magnetometer works on the principle of gating the ambient field by modulating the permeability of a piece of magnetic material through the application of an alternating gating field. The resultant modulated ambient field is an even function of the gating field, and the voltage induced in a signal coil which links these fluctuating flux fields contains the fundamental frequency of the gating field and the even harmonics of the gated ambient field. In order to detect an ambient field of the order of 0.1γ a stable rejection factor for the fundamental frequency of the order of 10^{-9} would be needed, because the gating field density for most magnetic materials is of the order of $10^{8}\gamma$. The standard technique is to employ the method of direct bucking

Presented as Preprint 63-187 at the AIAA Summer Meeting, Los Angeles, Calif., June 17–20, 1963; revision received January 6, 1964.

* Head, Experimental Section; now Research Associate Professor, Department of Space Sciences and Applied Physics, Catholic University of America, Washington, D. C. This work was carried out on behalf of NASA, under contract NASr-46, with the Center for Radiophysics and Space Research of Cornell University. The author wishes to thank T. Gold for his general guidance on this project and H. S. Tan for his invaluable advice and inspiration. Acknowledgment is also due to H. Eckelmann for his assistance in experimental investigations and circuit design.

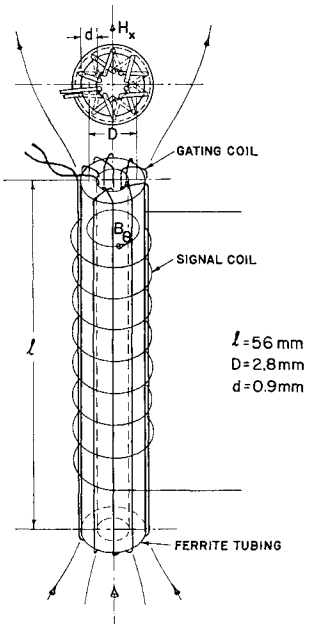

Fig. 1 Axially symmetrical fluxgate sensor.

of the fundamental frequency by means of two precisely matched and aligned pairs of sensors,[1] and to remove the residual fundamental frequency by a sharp cutoff filter or tuned amplifiers. Although a rejection factor of the order of 10^{-9} can be realized in the controlled environment of a laboratory, it is questionable that the critical 10^{-5} balance of the bucking system can be maintained under space environment, because both systems are pushed beyond the practical limit of 10^{-3}, and, in addition, neither system can reject random noise within the passband of the filter.

A search was therefore made for combinations of physical properties which might lead to an improvement of the rejection factor. It was found that by combining properties of the material due to its physical structure and geometry, a magnetometer with a self-decoupling factor of the order of 10^{-7} is realized. The term decoupling factor is defined as the fraction of the total gating-flux field that is linked with the signal coil. This method, based on the minimum flux linkage between the gating field and the ambient field, is superior in many respects to the direct bucking principle just mentioned. In the following sections, detailed properties and theories of this improved magnetometer will be discussed.

Physical Principles

The physical arrangement of an axially symmetrical magnetometer is shown in Fig. 1. The magnetic core is in the form of small ferrite tubing with a large length-to-diameter ratio. A toroidal gating coil is wound through the tubing. In order to achieve a zero net winding pitch with one layer of winding, all wires along the ferrite tubing are kept parallel to the mechanical axis and the winding pitch is taken up at the ends of the tubing. The end winding pitches are crisscrossed to achieve zero net pitch. A signal coil is wound in the form of a solenoid coaxial with the ferrite tubing and perpendicular to the gating coil. This winding consists of even number of layers, so as to obtain a zero net winding pitch. To reduce electrostatic coupling, an electrostatic shield is placed in between the gating coil and the signal coil. The assembly is then mounted with sliding end-supports inside a precision quartz tube. This method of suspension minimizes stresses due to external load and thermal expansion.

Large decoupling factors, based on the principle of minimum flux linkage between the gating field and the ambient field, can be achieved by the combination of several physical and geometrical properties. The first step is to apply the bottling property of a toroidal coil: All of the field generated by a toroidal coil is confined within the toroid if the net winding pitch is zero.[2] Next is the utilization of the property of precise orthogonality between the gating and the signal coil. The last important step is to place within the toroidal coil a magnetic material that has a preferred direction of magnetization in the circumferential θ direction, i.e., in the H_θ field direction of the gating coil. From the geometric shape of the ferrite tubing it can be shown that the θ direction is the easiest direction of magnetization, because in this direction the magnetic path is the shortest and closed so that there is no external demagnetization field. The effective magnetic reluctance in the θ direction, ρ_θ, can be expressed in terms of its geometry and the initial permeability of material μ_0:

$$\rho_\theta = \pi D/\mu_0 dl \tag{1}$$

where D is the mean tube diameter, d the wall thickness, and l the length of tube. The next easy direction of magnetization is along the axial direction. Here the external demagnetization field has to be taken into consideration, and the effective reluctance in the axial direction ρ_r is

$$\rho_r = \frac{4l}{\mu_r[(l/D),\mu_0]\pi D^2} \tag{2}$$

where μ_r, the apparent permeability of tube, is a function of l/D ratio and μ_0. The function can be found in published data.[3] Portions of the data useful for the present work are replotted in Fig. 2.

To achieve a high decoupling factor, the ratio of reluctances,

$$\frac{\rho_\theta}{\rho_r} = \frac{\mu_r[(l/D),\mu_0]\pi^2 D^3}{4\mu_0 dl^2} \tag{3}$$

must be made as small as possible.

If l/D is made large, the reluctance ratio can be made very small. In the present design, the ratio of reluctance is of the order of 10^{-3}. Combining this ratio with that of the minimum coupling property of the signal and gating coils, a decoupling factor of the order of 10^{-7} has been obtained and verified by experiment. (A magnetometer constructed with only normal care will give a decoupling factor of the order of 10^{-6}, but one built with due care and adjustment can give 10^{-7}.) In order to obtain a total of 10^{-9}, the remaining factor of 10^{-2} is obtained by a standard filtering technique.

The axially symmetric gating field in the form of a toroid contributes to certain important properties. The H_θ field within the ferrite tubing is quite uniform; hence, all of the

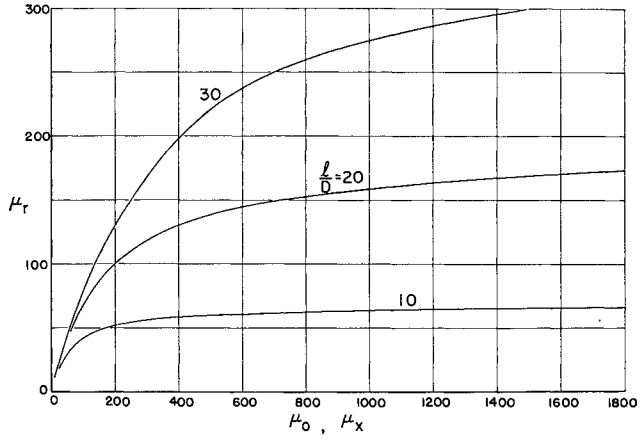

Fig. 2 The apparent permeability of a rod in an external field as a function of permeability of material.

material is subjected to uniform saturation by an alternating gating field, and the possibility of retaining a large residual magnetism, after subjecting the magnetometer to a strong ambient field, is greatly reduced. Experimental results have indicated that after the magnetometer is subjected to a field less than saturation it can recover to its original level practically instantaneously. For field strengths greater than saturation, its recovery time is greatly increased to the order of minutes. On the other hand, the minimum leakage of gating flux and flux coupling between the orthogonal coils have essentially decoupled the random noise (one component of the Barkhausen noise), generated by the gating field, from the signal coil. If the noise field is assumed to be essentially in the θ plane, and its magnitude is much smaller than the average gating flux, the resultant noise voltage thus coupled into the signal coil is expected to be several orders smaller than the minimum signal to be detected. The low-frequency components of Barkhausen noise usually produce undesirable low-level signal drift.[4] The complete decoupling of this effect on the present design is an important contribution toward the stability of the zero level.

This type of magnetometer can provide very large signal outputs; with proper coil design and driving circuitry, signals of the order of few millivolts per gamma are typically produced. At this output level, there is, in general, no need for any further voltage amplification. The signal-coil output impedance is of the order of 10^5 ohms, so that a common collector transistor circuit can be used to transform the output impedance to the order of 10^2 ohms, without significant loss in output signal. At this impedance and signal-output level, the problems of coupling of stray signals and the stability of associated processing circuitry are greatly alleviated. The resultant simplicity of supporting circuitry should, as a rule, enhance the over-all reliability of the magnetometer. Further, it is insensitive to mechanical vibration, because of its new gating principle (quite different from the standard direct-bucking principle that relies on the absolute symmetry of two large signal sources under all disturbing environmental variables and conditions). It is important to note that the principle of self-decoupling factor, based on minimum flux linkage, automatically reduces the environmental variables by a large factor, and thus eliminates all delicate balancing and matching operations.

General Theory of Fluxgate

Principle of Fluxgate

The principle of orthogonal gating is not new, the general theory having been advanced by Zhukova,[5] Gorelik,[6] and Palmer.[7] Most of their works are intended for wire-type magnetometers in which the gating current through the magnetic wire creates its own circular saturating field, while the ambient field or its component is lined up with the wire axis. Although considerable effort has been put on this

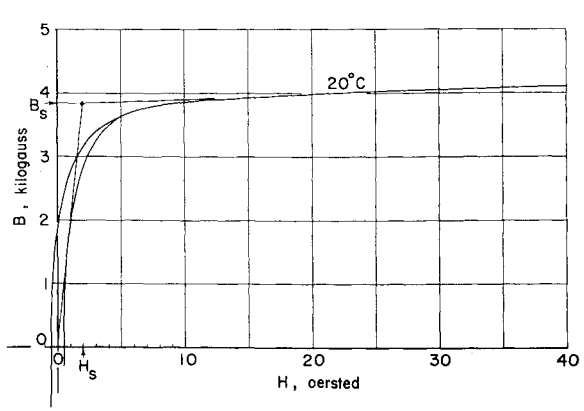

Fig. 3 *B-H* curve for type A-3 manganese-zinc ferrite.

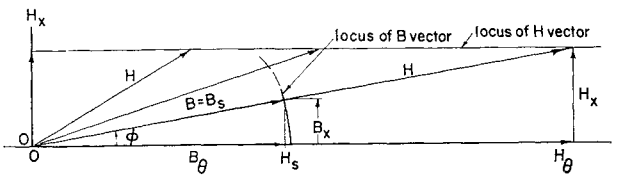

Fig. 4 Vector diagram of *B* and *H* field beyond saturation.

subject, there is as yet no exact theory that can fully account for gating characteristics observed experimentally. The reason is that most magnetic materials are not isotropic. They also exhibit hysteresis which, under a rotating magnetizing field, is as yet intractable analytically. This paper does not attempt to go into detail in the solid-state physics of magnetic materials, but will touch upon some phenomenological theories of orthogonal gating which lend reasonable explanations for the gating mechanism.

The object here is to find out the functional relationship between the apparent axial permeability of the magnetometer μ_r and the orthogonal gating field H_θ. It is expedient to refer μ_r to the differential permeability of the magnetic materials μ_x in the same axial direction. The apparent permeability μ_r is a function of μ_x and geometry. Their functional relationship is shown in Fig. 2 for a cylindrical rod. This function also may be considered valid for thick-walled tubing used in the present problem.

The functional relationship between μ_x and the orthogonal gating field H_θ cannot be fully accounted for by the present theories. The standard B-H characteristics of one dimension are not applicable to a rotating H field. However, for a field strength H above saturation H_s, we may assume the B vector to be colinear with the H vector.[8] For simplicity of presentation, H_s and B_s are defined as the knee point of two straight lines which represents the B-H curve of a given material, as shown in Fig. 3. Figure 4 shows the vector diagram of the resultant H vector for a varying orthogonal gating field H_θ and a small steady axial field H_x. For the present application, H_x is of the order of 10^{-7} of the average gating field H_θ. Therefore, for $H_\theta \gg H_s$ one may take $|H|$ to be the same as $|H_\theta|$ and the resultant $|B|$ to be equal to $|B_\theta|$. When the H field is greater than H_s, the B vector reaches the limit of saturation density B_s, and the locus of the B vector is an arc described by B_s, as the angle ϕ of the total H vector reduces with increasing H_θ. From the vector diagram, we see that the component of B_x is approximately

$$B_x \doteq H_x \frac{B_s}{H_\theta} \doteq \left(\mu_0 \frac{H_s}{H_\theta}\right) H_x \qquad H_\theta \gg H_s \tag{4}$$

or

$$\mu_x/\mu_0 \doteq H_s/H_\theta \tag{5}$$

When the peak value of H_θ is 20 times H_s, μ_x is reduced to 5%, or a gate closure of 95%. However, in actual case, the closure was found to be about 85% for a typical magnetometer, as shown in Fig. 5.

On the right-hand side of Fig. 5 is the experimental curve of apparent permeability $\mu_r/\mu_{r\,\max}$ as a function of H_θ/H_s. This is obtained by measuring the change in inductance of the signal coil as a function of H_θ. The ratio $\mu_r/\mu_{r\,\max}$ is slightly less than unity at $H_\theta = 0$, and there is a small hysteresis loop around this region. An important property of orthogonal gating, as shown here, is that μ_r does not exhibit any double peaking effect as those associated with parallel gating.[9] This means that the magnetic retentivity in the axial direction due to the strong orthogonal gating field is negligibly small. Through the known relationship between μ_x and μ_r (see Fig. 2), the functional relationship between μ_x and H_θ is plotted on the left-hand side of Fig. 5. It will be noted that the closure of apparent permeability μ_r is much less than μ_x.

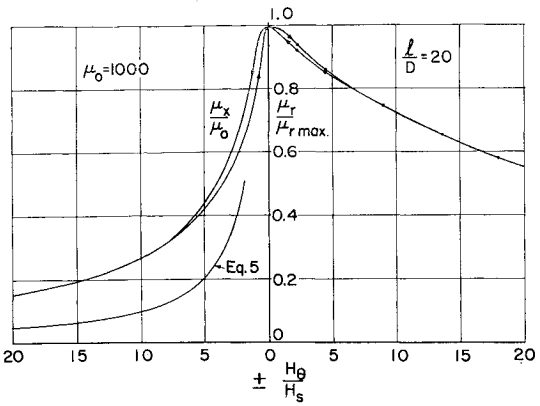

Fig. 5 Apparent permeability of tubing and axial permeability of material as a function of H_θ/H_s.

In the present design, it is arbitrarily decided to use a peak gating-field strength of $H_\theta = 20H_s$, since higher gating fields will run into uneconomical power consumption and heat-removal problems. At this gating level, one is assured of quick pulldown of any large residual magnetism that the magnetometer might have acquired during operation.

When we drive the magnetometer at a high H_θ/H_s ratio, we have to operate the gating coil as a highly nonlinear inductor. The problem then is to find the best over-all driving characteristic for this inductor so as to produce maximum signal with minimum noise and power consumption. In the present design, the gating coil is connected in parallel with a condenser to form an oscillating tank so that, during the saturation period, the condenser is capable of dumping high current into the coil to produce the large peak H_θ field required for gating operation.

The fundamental self-relaxation frequency of the tank is approximately

$$f_g \doteq E_g/2L_gI_s \tag{6}$$

where E_g is the average peak voltage across the tank between gating cycle, L_g is the average initial inductance of the gating coil, and I_s is the current required for saturating the inductor. From the consideration of transistor drive, the average peak tank voltage in the present design is limited to 4 v, or 8 v peak-to-peak. The gating coil contains 14 turns of #28 wire to give an L_g value of about 1.5 mh. The current I_s required is about 0.1 amp. With these values for Eq. (6), we obtain a relaxation frequency f_g of about 10 kc/sec.

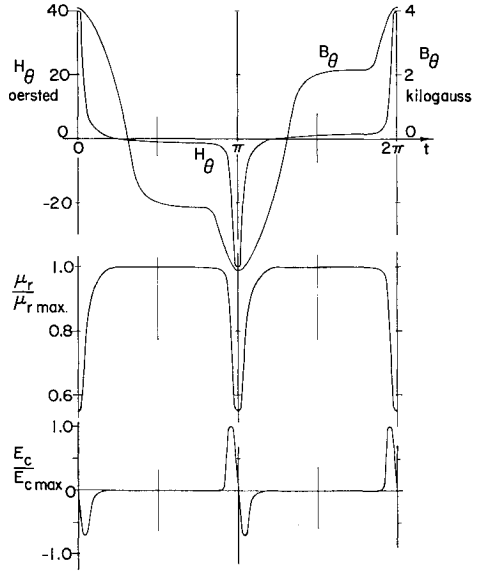

Fig. 6 Periodic wave forms of gating field, apparent permeability, and damped output signal.

There are two possible methods for driving the gate. One is to connect the tank in a transistor drive circuit to form a self-relaxation oscillator; the other is to drive it by an independent power oscillator with a frequency substantially lower than f_g. For various reasons the latter method was adopted, and a driving frequency of 5.5 kc/sec was used.

Figure 6 shows the gating current, or rather the gating field H_θ, as a function of time. No attempt will be made to present the complex solution for this function in relationship to the tank and its drive circuit since analytical treatment on this subject has been made by Ku.[10] The gating wave of the present design is in the form of very sharp alternating pulses with a peak current of about 2.2 amp, or a field strength of about 40 oe. The I^2R power loss is about 0.15 w, where R is the resistance of the gating coil and cable leads; the hysteresis loss in the ferrite tubing is of similar magnitude, so that the total gating loss for the sensor is about 0.3 w.

Also shown in Fig. 6 is the gating flux B_θ. This curve is highly distorted due to hysteresis. The corresponding gating of ambient-flux field, shown in terms of $\mu_r/\mu_{r\,max}$ in the lower part of the figure, was obtained through the functional relationship between μ_r and H_θ (Fig. 5). It is interesting to note that due to hysteresis, μ_r closes, or decreases, a little faster than when it is opening. The closure rate depends largely on the initial rate of rise of the H_θ pulse. The output voltage across the signal coil is proportional to the time derivative of $B_r(t)$ or, in turn, the time derivative of $\mu_r(t)$. By taking the time derivative of the $\mu_r/\mu_{r\,max}$ curve, we obtain the voltage wave which is plotted as $E_c/E_{c\,max}$ in Fig. 6. It will be noted that this signal wave is unsymmetrical about the zero line and that it contains the second and higher harmonics of the fundamental gating frequencies. It is evident that a better and cleaner second harmonic signal can be obtained if the gating action were timed evenly at the quarter phase points, but this will require unduly wide H_θ pulses which, in turn, means very large I^2R loss.

The signal coil in the present design contains about 1600 turns of #36 wire, and is tuned to the second harmonic by a condenser in parallel with the coil. The Q of the coil is about 40, so the output voltage E_2 across the tuned tank is about Q times the second-harmonic signal component of E_c:

$$E_2 = K_2E_cQ \tag{7}$$

where K_2 is the coefficient of second harmonic of E_c.

Spectrum of Transverse Induction

So far we have treated the problem of an ideal magnetometer, ignoring inhomogeneity of magnetic materials, nonsymmetry in geometrical shape, and stresses due to externally applied load or internally generated stress. Now we must find out how these variables will affect the output signal in terms of the various frequency components. We shall consider the magnetic materials to be nonisotropic; the general expression for the permeability tensor is $\underline{\mu}(H_\theta, H_x, \sigma; \text{sign}\dot{H}_\theta)$. We shall consider H_x and the principle stress σ to be fixed parameters, while H_θ is a periodic function of time, $H_\theta = H_{\theta_0}e^{i\omega t}$.

The transverse or axial induction B_x, due to the gating action of H , is also a periodic function of time, and it can be expressed in the general form

$$B_x = \mu_{xx}(H_\theta, H_x, \sigma; \text{sign}\dot{H}_\theta)H_x + \mu_{x\theta}(H_\theta, H_x, \sigma; \text{sign}\dot{H}_\theta)H_\theta \tag{8}$$

The permeability tensor can be written as the sum of triple power series. Following the method of Zhukova,[5] which is based on the consideration of symmetry, we have the ex-

pression for B_x:

$$B_x(t) = \Sigma\alpha_{mnp}H_\theta^{2p}H_x^{2m+1}\sigma^{2p} + \Sigma\beta_{mnp}H_\theta^{2n+1}H_x^{2m}\sigma^{2p+1} \pm \Sigma\zeta_{mnp}H_\theta^{2n+1}H_x^{2m+1}\sigma^{2p} \pm \Sigma\delta_{mnp}H_\theta^{2n}H_x^{2m}\sigma^{2p+1} \quad (9)$$

where α, β, ζ, and δ are coefficients. The hysteresis loop is expressed by the bivalued function. The $\pm$ sign is to be taken as positive when $\partial H_\theta/\partial t > 0$, and negative when $\partial H_\theta/\partial t < 0$. It can be shown that the bivalued function makes odd functions of H_θ even, and even functions of H_θ odd. The basic effect of hysteresis is to cause a small phase shift to all of the frequency components. In general, the first and third right-hand terms of the previous expression represent the second and higher even harmonics of H_θ, whose coefficients are odd functions of H_x, and even functions of σ, whereas the second and fourth terms represent the fundamental and higher odd harmonics of H_θ whose coefficients are even functions of H_x and odd functions of σ. Since the second and fourth terms represent the undesirable leakage flux, we shall designate them the "leakage magnetism."

In operation, all frequencies except the second-harmonic component are filtered out. The contribution of second-harmonic component due to small H_x and σ is proportional to

$$H_x(1 + a\sigma^2)$$

where a is a constant. The amplitude of B_x is therefore a linear function of H_x, and its phase position is determined by the sign of H_x alone, and not by H_θ nor σ. The contribution due to σ is not objectionable as long as $a\sigma^2 \ll 1$ and stays constant.

The contribution of fundamental-frequency component for small H_x and σ is proportional to

$$\sigma(1 + bH_x^2)$$

where b is a constant. If the gating field H_θ contains no second harmonic, there is no contribution of second-harmonic signal by this term. However, if the reverse is true, then the second harmonic contributed by this term is quite undesirable because it is an even function of H_x. Its effect is equivalent to a permanent magnetism whose phase position is independent of the sign of H_x. It is, therefore, quite important to have minimum second-harmonic component in H_θ. However, in the present design, due to the inherent self-decoupling factor, a maximum second-harmonic content of 0.1% of the fundamental component of H_θ is considered acceptable (i.e., equivalent to a signal level of 0.01γ).

The "leakage magnetism" can be detected at the output of the signal coil by reversing the polarity of H_θ. The second-harmonic component that changes sign with H_θ is the "leakage magnetism" since it is an odd function of H_θ.

Electronic Circuits

From the previous discussion of the basic principle of the sensor, one sees that there are many ways of driving the fluxgate, as well as processing its output signal. In this paper one basic design is presented.

In general, the sensor is to be incorporated in a self-balancing (or servo) system in which a current is fed back into the signal coil, or a separate secondary coil, to balance out the ambient field. The feedback current is then calibrated as a function of the ambient field. In this mode of operation, one achieves minimum disturbance to the ambient field because the magnetic reluctance ρ_r is increased by a factor of 1000, on account of the suppression factor of the servo. This then will permit the placement of three orthogonally oriented sensors in close proximity and free from the effect of interreaction.

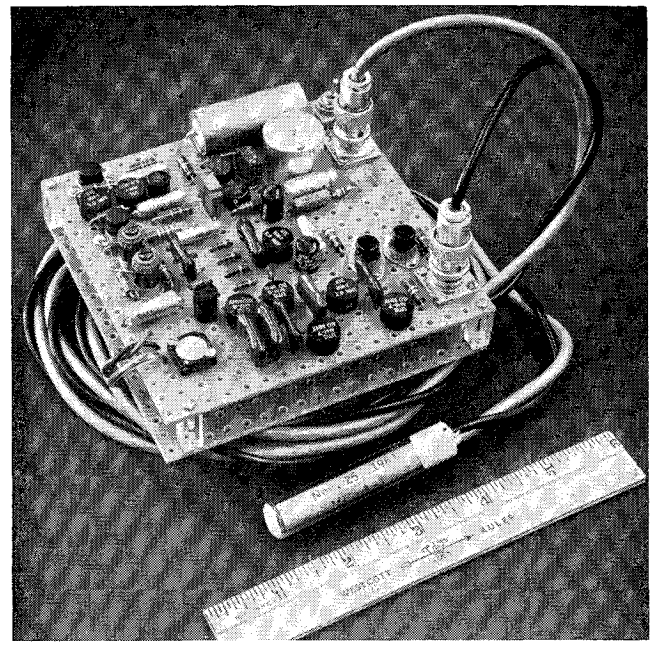

Fig. 7 Breadboard model of the fluxgate magnetometer.

Because of the limitation of space, the servo system and the three-component vector-type magnetometer will be presented in a separate paper. Here we shall discuss only a very simple transistorized driver and signal detecting circuit. Figure 7 shows the breadboard model of the magnetometer; the corresponding circuit diagram for the magnetometer is presented in Fig. 8.

The Driving Circuit

The driving circuit for the magnetometer consists of three sections: the regulator, the oscillator, and the power driver. The regulator Q_1 regulates the bias of the push-pull oscillator, Q_2 and Q_3, and thus controls its output amplitude. The error signal for the regulator is derived through the rectifying

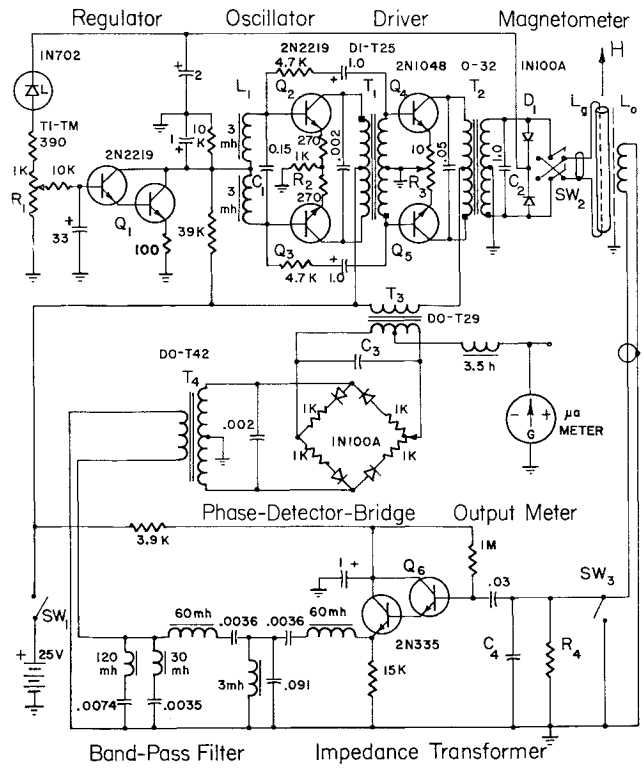

Fig. 8 Circuit diagram.

diedos D_1 across the gating coil of the magnetometer, and the trimpot R_1 is used for setting the regulator to control the peak gating current at 2.2 amp. The frequency of the oscillator is determined by the L_1C_1 tank circuit, which is tuned to 5.5 kc/sec. The large common-emitter resistor R_2 provides the automatic suppression of second harmonic. The power drivers Q_4 and Q_5 are operated in a class B condition for minimum power consumption, and each dissipates approximately $\frac{1}{4}$ w. The transformer T_2 is used for matching the impedance of the magnetometer to the power driver. Condenser C_2 is the tank capacitor for the gating coil L_g. Its value is chosen to provide the desired gating wave form as shown in Fig. 6.

In operation, when the power switch SW_1 is turned on, the gating current is zero. The regulator is biased to cutoff and the oscillator is allowed to run at its maximum amplitude, which is almost twice the value necessary for starting the magnetometer into its saturation cycles. As soon as this happens, the regulator starts to pull the oscillator down to run at a preset running level. This happens because it takes more energy or voltage to start the magnetometer than it is necessary to run at an economical level once the saturation cycle is initiated. Should the magnetometer stop running for some reason, the regulator will automatically perform the restarting procedure. The regulator circuit shown here is intended for illustrative purposes. In actual design, a more complex circuit with positive temperature compensation is used.

The Signal Circuit

Before the output from the signal coil of the magnetometer is fed into the signal processing circuit it is shunted by a capacitor and a resistor. The capacitor C_4 is used for tuning the signal coil to the second harmonic, and the resistor R_4 is to provide the extra damping required by the L_0C_4 tank to prevent it from going into parametric oscillation. The signal circuit consists of three basic sections: the signal impedance transformer, the filter section, and the phase-detector-bridge.

The common collector circuit of Q_6 transforms the output impedance of the tuned signal coil from a level of 10^5 ohms to an output level of 100 ohms. Following Q_6 is a sharp bandpass filter, whose passband is 10–12 kc. The maximum cutoff frequencies occur at the fundamental (5.5 kc) and the third harmonic (16.5 kc) with a maximum attenuation of -40 db.

The phase-detector bridge derives its reference signal from the second-harmonic current pulses of the class B power driver. The primary winding of transformer T_3 is connected in series with the power supply and transformer T_2, and its secondary winding is tuned to the second harmonic by capacitor C_3. The reference voltage for the phase-detector bridge is derived from this output. The output signal from the filter section is coupled into transformer T_4 to provide a balanced output required for the detector. The detected d.c. signal between the center tapes of T_4 and T_3 is shunted by a 3.5-h choke, and an output indicating microammeter with a total load resistance of 2000 ohms.

The double-pole double-throw switch SW_2 at the output of T_2 is used for reversing the polarity of the gating current. Switch SW_3, at the output of the signal coil, is to be used in conjunction with SW_2, so that it is grounded whenever SW_2 is to be switched, and opened again when the switching operation is completed. In this manner, the switching operation induces a strong oscillating current in the signal coil, which tends to urge any residual field in the sensor toward a reproducible zero level of 0.1γ. The purpose of SW_2 is the detection of the "leakage-magnetism" component as discussed previously; the trimpot R_3, connected to the emitters of the power driver, is used for adjusting the "leakage magnetism" to a minimum value.

The total power consumption of the magnetometer is about 1.2 w. With a more efficient driver circuit, a power drain of 0.9 w can be achieved. The magnetometer was calibrated in a zero-field tank. The output sensitivity was found to be about 3 mv/γ, and it is linearly related to the ambient field within experimental accuracy. No hysteresis was observed on the calibration curve.

Problems relating to the long-term stability of the magnetometer depend, to some extent, on the stability of its controlling circuits. Since more advanced driver circuits and servo systems will be treated in a separate paper, the discussion of this important problem will have to be deferred until then.

Conclusion

The main emphasis of this paper is to present the technique and theory by which a low-level magnetometer is developed for space application; therefore, no attempt was made to discuss magnetometers which involve more complex electronic circuitries. A simplified phenomenological theory was presented to explain the general mechanics of an orthogonal fluxgate, and, in addition, the general characteristic of the spectrum of transverse induction was discussed. Specifically, we have developed a sensor that has the following attributes: 1) high signal output, such that further amplification of the signal is generally unnecessary; 2) decoupling of the gating field and the associated component of Barkhausen noise from the signal field; 3) minimization of hysteresis on the output signal; and 4) freedom from drift due to mechanical vibration and temperature change. All of these factors contribute toward a clean, sharp, and stable null at the zero field-level of 0.1γ— a principal parameter which determines the limiting quality of a self-balancing magnetometer.

References

[1] Kuhne, R., "Magnetfeldmessung mit Eisenkern-Magnetometer nach dem Oberwellenverfahren," Arch. Tech. Messen **V392-1**, 175 (August 1952).

[2] Seely, S., *Introduction to Electromagnetic Fields* (McGraw-Hill Book Co., Inc., New York, 1958), p. 170.

[3] Bozorth, R. M., "Demagnetizing factor of rods," J. Appl. Phys. **13**, 320 (1942).

[4] Williams, F. C., "The fundamental limitations of the second-harmonic type of magnetic modulator as applied to the amplification of small d.c. signals," Proc. Inst. Elec. Engrs. (London) **II97**, 445 (August 1950).

[5] Zhukova, I. M., "Concerning the spectrum of e.m.f. of transverse induction," Dokl. Akad. Nauk SSSR **65**, 151 (1949).

[6] Gorelik, G., "Surles courbes d'aimantation longitudinal dún fil ferromagnetique parcouru par un courant continu," Compt. Rend. (Dokl.) Acad. Sci. URSS **XLIV**, 235 (1944).

[7] Palmer, T. M., "A small sensitive magnetometer," Proc. Inst. Elec. Engrs. (London) **100**, 545 (1953).

[8] Shamos, M. A., *Recent Advance in Science* (Science Editions Inc., 1961), p. 273.

[9] Smit, J., *Ferrites* (John Wiley & Sons, Inc., New York, 1959), p. 261.

[10] Ku, Y. H., *Analysis and Control of Nonlinear System* (Ronald Press Company, New York, 1958), p. 226.